GB04/1676

**INVESTOR IN PEOPLE**

## PRIORITY DOCUMENT

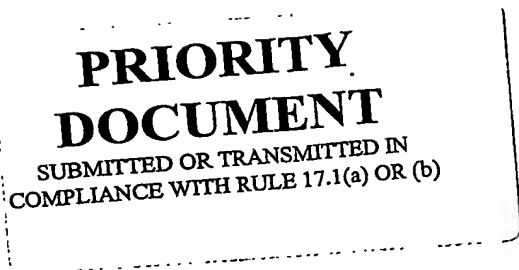SUBMITTED OR TRANSMITTED IN COMPLIANCE WITH RULE 17.1(a) OR (b)

The Patent Office
Concept House
Cardiff Road
Newport
South Wales
NP10 8QQ

REC'D **17 MAY 2004**

WIPO                    PCT

I, the undersigned, being an officer duly authorised in accordance with Section 74(1) and (4) of the Deregulation & Contracting Out Act 1994, to sign and issue certificates on behalf of the Comptroller-General, hereby certify that annexed hereto is a true copy of the documents as originally filed in connection with the patent application identified therein.

In accordance with the Patents (Companies Re-registration) Rules 1982, if a company named in this certificate and any accompanying documents has re-registered under the Companies Act 1980 with the same name as that with which it was registered immediately before re-registration save for the substitution as, or inclusion as, the last part of the name of the words "public limited company" or their equivalents in Welsh, references to the name of the company in this certificate and any accompanying documents shall be treated as references to the name with which it is so re-registered.

In accordance with the rules, the words "public limited company" may be replaced by p.l.c., plc, P.L.C. or PLC.

Re-registration under the Companies Act does not constitute a new legal entity but merely subjects the company to certain additional company law rules.
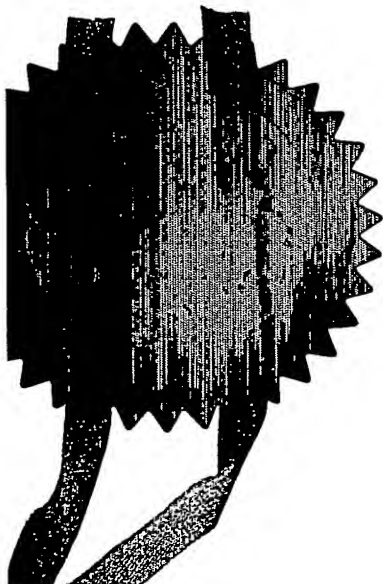
Signed

Dated      6 May 2004

An Executive Agency of the Department of Trade and Industry

THE PATENT OFFICE
PS
**2 3 APR 2003**
RECEIVED BY FAX

**Patents Form 1/77**

Patents Act 1977
(Rule 16)

**The Patent Office**

23APR03 E801845-1 D02973
P01/7700 0.00-0309142.8

# Request for grant of a patent

*(See the notes on the back of this form. You can also get an explanatory leaflet from the Patent Office to help you fill in this form)*

**2 3 APR 2003**

The Patent Office

Cardiff Road
Newport
South Wales
NP9 1RH

1. Your reference

   **P102426AGB**

2. Patent application number
   *(The Patent Office will fill in this part)*

   **0309142.8**

3. Full name, address and postcode of the or of each applicant *(underline all surnames)*

   DSTL Abbey Wood
     Poplar 2
   MOD (DPA) Abbey Wood #19
   BRISTOL BS34 8JH

   Patents ADP number *(if you know it)*

   If the applicant is a corporate body, give the country/state of its incorporation    GB     *8182297003*

4. Title of the invention

   Tropospheric Delays in Global Positioning Systems

5. Name of your agent *(if you have one)*    Harrison Goddard Foote

   "Address for service" in the United Kingdom to which all correspondence should be sent *(including the postcode)*

   Orlando House
   11c Compstall Road
   Marple Bridge
   Stockport SK6 5HH
   United Kingdom

   Patents ADP number *(if you know it)*    *GB14571002*

6. If you are declaring priority from one or more earlier patent applications, give the country and the date of filing of the or of each of these earlier applications and *(if you know it)* the or each application number

   Country    Priority application number *(if you know it)*    Date of filing *(day / month / year)*

7. If this application is divided or otherwise derived from an earlier UK application, give the number and the filing date of the earlier application

   Number of earlier application    Date of filing *(day / month / year)*

8. Is a statement of inventorship and of right to grant of a patent required in support of this request? *(Answer 'Yes' if*
   a) *any applicant named in part 3 is not an inventor, or*
   b) *there is an inventor who is not named as an applicant, or*
   c) *any named applicant is a corporate body.*
   *See note (d))*

   Yes

Patents Form 1/77

ts Form 1/77

nter the number of sheets for any of the
following items you are filing with this form.
Do not count copies of the same document

Continuation sheets of this form

Description    16 ✓

Claim (s)    3

Abstract

Drawing (s)

10. If you are also filing any of the following,
state how many against each item.

Priority documents

Translations of priority documents

Statement of inventorship and right
to grant of a patent *(Patents Form 7/77)*

Request for preliminary examination
and search *(Patents Form 9/77)*

Request for substantive examination
*(Patents Form 10/77)*

Any other documents    1    Covering letter
*(please specify)*

---

11.    I/We request the grant of a patent on the basis of this application.

Signature *Harrison Goddard Foote*    Date

Harrison Goddard Foote    23 April 2003

---

12. Name and daytime telephone number of
person to contact in the United Kingdom    Roger Henderson    0161 427 7005

---

**Warning**

*After an application for a patent has been filed, the Comptroller of the Patent Office will consider whether publication or communication of the invention should be prohibited or restricted under Section 22 of the Patents Act 1977. You will be informed if it is necessary to prohibit or restrict your invention in this way. Furthermore, if you live in the United Kingdom, Section 23 of the Patents Act 1977 stops you from applying for a patent abroad without first getting written permission from the Patent Office unless an application has been filed at least 6 weeks beforehand in the United Kingdom for a patent for the same invention and either no direction prohibiting publication or communication has been given, or any such direction has been revoked.*

**Notes**

a) *If you need help to fill in this form or you have any questions, please contact the Patent Office on 0645 500505.*

b) *Write your answers in capital letters using black ink or you may type them.*

c) *If there is not enough space for all the relevant details on any part of this form, please continue on a separate sheet of paper and write "see continuation sheet" in the relevant part(s). Any continuation sheet should be attached to this form.*

d) *If you have answered 'Yes' Patents Form 7/77 will need to be filed.*

e) *Once you have filled in the form you must remember to sign and date it.*

f) *For details of the fee and ways to pay please contact the Patent Office.*

Patents Form 1/77

## Global Positioning Systems

The present invention relates to developments intended to increase the accuracy obtainable from global navigation satellite systems (GNSS).

5    At present there are two publicly available GPS systems, known as NAVSTAR, owned by the USA, and GLONASS owned by the Russian Federation. These have been in existence for around two decades, but in the near future it is hoped that the European regional augmentation of GPS will start to provide its services, followed within a few years by a European system under the name of GALILEO.

The existing systems have been progressively refined so that using a differential phase
10    implementation a locational accuracy of less than 2 cm can potentially be achieved over a baseline of 1000 km, but with a cost in computation and in the time taken to determine the location. Real time or near real time measurements have a correspondingly lower resolution, and at present the requirements for high precision mean that additional augmentations are necessarily employed to supplement the
15    GNSS information. Furthermore, these could include a receiver taking measurements from many satellites, up to all those visible to it whereby to calculate an over-determined position solution and rejecting inconsistent data to improve the accuracy of the position solution. Such a system may use data from more than one constellation of GNSS satellites, GPS and GLONASS. However, a significant error arises from the
20    inability to model accurately the delay to the GNSS signals caused by the troposphere.

One of the largest identified sources of error lies in the effect that the troposphere has on signals propagating therethrough. The troposphere introduces ray bending and a signal delay which is influenced by a number of meteorological factors, but particularly water content.

25    Traditionally, this delay has been handled by the use of global tropospheric delay models. This weather data is too large to be sent over communication systems that are available to mobile users.

1

However, recently an attempt has been made to introduce numerical weather prediction (NWP) into the GPS process, whereby local estimates of tropospheric delay can be provided. The intention was to use high resolution NWP for determining the tropospheric zenith delays for the estimated position of a GPS

5 receiver, instead of using a global delay model, which delays can subsequently be used in the positioning process.

However, even if the zenith delay is known, there will be a need for a user to be able to correct for other directions if increased accuracy of measurement is desired.

The present invention provides a method of obtaining data for use in a satellite

10 positioning system or GNSS comprising the steps of generating a first set of less accurate tropospheric delay values from a first model which is known per se, the first model being based on a first set of parameters, generating a second set of more accurate tropospheric delay values from a second model based on meteorological information, and developing a modified said set of parameters for use with said first

15 model so that it then provides a set of delay values substantially approximating the second set, and expressing at least one of said modified set of parameters as a correction parameter for communication to a user.

In an embodiment of the invention, these parameters are differences with those obtained from the first model and are transmitted to the receiver.

20 In one embodiment the first model is based on one or more non-meteorological parameter(s). These parameter(s) comprise at least one of (A) time of year, (B) latitude and (C) altitude to generate an estimate of the zenith tropospheric delay.

As particularly described, the non-meteorological parameters are employed for determining a mapping function relating tropospheric delay at a given elevation angle

25 to the zenith delay generated by this first model. A mapping function using a continued fraction function based on the three non-meteorological parameters such as used by Niell may be used for this process of generating the mapping function.

2

The second model may be based on NWP or real time meteorological data, which is used to calculate the zenith tropospheric delay. Currently the cell size of NWP data is of the order of 12 km, but this is expected to reduce in the future allowing finer determination of the model and mapping function. Using the NWP or other

5   meteorological data (collectively NWPO) a ray tracing technique is used to determine the path of the satellite signal through the troposphere to the user and hence estimate the delay from a direct path. Knowing the delay, a second set of mapping function parameters may be derived by fitting the results to the format of the mapping function used in the first model.

10  Recognising that the two models have generated two values for the same set of parameters, it is only necessary to communicate to the user the differences in the form of corrections (e.g. as actual numerical differences, or as a multiplier of the value in the first model) to the four parameters estimated (zenith delay and the three parameters used to generate the mapping function) in the first model, although it

15  would be possible to communicate the parameters generated by use of the second model.

Depending on the non-homogeneity of the troposphere it may only be necessary to generate a subset of the parameters although the most important is the zenith delay followed in order by A, B and C.

20  To be of use the data must be communicated to the user within the time for which the NWPO is valid. As noted above the NWP data is defined over a geographic grid. If the standard deviation for the change in zenith delay for a cell in the grid in a period t equals the inaccuracy in the second set, then for a workable system (where the measurement period is less than changes in tropospheric conditions leading to

25  misleading results) the data reduction needs to be effective to reduce the data to an amount which can be transmitted over the capacity of the data link in a time t' substantially less than t, and preferably no more than t/4.

The derived correction parameters are distributed according to location over at least part of the earth's surface and may be communicated to at least one geostationary or

3

non-geostationary satellite or terrestrially based system. The GNSS satellites may also be used for this communications link. To enable the use of low capacity data links it is preferred to compress the distributed data prior to transmission. Such reductions may conveniently be performed using lossy image compression (such as

5    JPEG) or sub-sampling techniques.

Further details and advantages of the invention will be evident upon a reading of the appended claims, and upon a reading of the following article.

4

# Tropospheric Delay Modelling and Correction Dissemination using Numerical Weather Prediction Fields

Matthew Paws, James Butcher and John Owen
*Defence Science and Technology Laboratory*

## ABSTRACT

With the modernisation of GPS and the introduction of Galileo, tropospheric errors are to become an increasingly significant proportion of the GNSS user's error budget. This paper investigates the spatial and temporal properties of meteorological features on the tropospheric errors experienced by GNSS users. A regional real-time tropospheric correction service could be provided from refractivity profiles, derived from a numerical weather prediction model. An analysis is described of the bandwidth requirements for real-time tropospheric correction dissemination and of the trade-off between bandwidth and accuracy.

Whilst the dry atmosphere variability, both spatially and temporally is small, water vapour variability can be large. High-resolution mesoscale numerical weather fields enable analysis of the abrupt spatial and temporal changes of atmospheric moisture associated with weather fronts. A three-dimensional ray-tracing technique has been developed to compute tropospheric delays from mesoscale numerical weather prediction fields for defined satellite elevation and azimuth angles. Quantified examples of abrupt spatial, including azimuthal, asymmetry and temporal tropospheric delay variability are given and statistical analysis of their likelihood presented.

Once the tropospheric delay can be established, the issue of the data compression of regional tropospheric information to form a practical service needs to be addressed. Different strategies for dissemination of regional tropospheric corrections are discussed and the trade-off between accuracy and correction service bandwidth described.

## 1. INTRODUCTION

Tropospheric delay corrections can be derived from a priori atmospheric model, an atmospheric model utilising real-time meteorological data or, given sufficient time, estimated from GNSS code and carrier observations.

This paper investigates the potential of Numerical Weather Prediction, NWP, models to provide tropospheric corrections.

The 3-D atmospheric profile information resulting from the process of numerical weather prediction offers the potential of providing a regional or global tropospheric correction service to GNSS users. In effect an accurate atmospheric refractivity field, and therefore tropospheric delay, is simply a by-product of the numerical weather prediction process. An accurate estimate of tropospheric delay can be obtained by ray-tracing through the refractivity field. The accuracy of a NWP-derived tropospheric correction is almost entirely dependent upon the ability to determine atmospheric water vapour content

## 2. 3D RAY TRACING

### 2.1 Propagation Theory

The speed of propagation of an electromagnetic wave through a medium can be expressed in terms of the refractive index, $n$, defined to be the ratio of the speed of light through free-space to the speed through the medium (Eq. 2-1).

$$n = \frac{c}{v} \qquad (2\text{-}1)$$

where:

$n$ is the refractive index
$c$ is the speed of light in free space
$v$ is the propagation velocity

The GNSS tropospheric time delay, ignoring relativistic effects, is defined to be the propagation time of the GNSS signal from the satellite to the user minus the free space propagation time:

$$d_{trop} = \int_{User}^{Sv} n(s)\,ds - \int_{User}^{Sv} ds \cdot \qquad (2\text{-}2)$$

$r$ is the distance along the propagation path. The first integral is along the curved propagation path; the second integral is along a geometric straight path.

The differential equation describing the curved ray path can be expressed, in cartesian coordinates, as [3]:

$$\frac{d}{ds}\left(n\frac{dr}{ds}\right) = \nabla n \qquad (2\text{-}3)$$

where   $r = r(s)$ is the vector describing the ray path,
   $s$ is the length of the curved ray path up to $r$,
   $n$ is the refractivity scalar field,
   $\nabla n$, a vector field, is the gradient of $n$.

The differential equation can be expanded as

$$\frac{d^2r}{ds^2} = \frac{1}{n}\left(\nabla n - \left(\nabla n \cdot \frac{dr}{ds}\right)\frac{dr}{ds}\right). \qquad (2\text{-}4)$$

A first order ordinary differential equation (ODE) with known initial values can be solved using numerical methods: for example Runge-Kutta or Adams-Moulton methods. Higher order differential equations can be solved numerically by rewriting them as an equivalent system of first order equations. Using the substitution $r_1 = r$ and $r_2 = r'$ (the first derivative), the ray path differential equation (2-4) can be expressed as an equivalent system of two first order differential equations 2-5 and 2-6:

$$r_1' = \frac{dr}{ds} = r_2 \qquad (2\text{-}5)$$

$$r_2' = \frac{d^2r}{ds^2} = \frac{1}{n}\left(\nabla n - (\nabla n \cdot r_1')r_1'\right) \qquad (2\text{-}6)$$

The determination of the ray path therefore amounts to the solution of a system of two ODEs with initial values. Matlab's function ode45 was used to solve the problem: a Runge-Kutta method with adaptive step control consistent with user defined tolerances.

The numerical weather prediction fields to be used are expressed in a spherical coordinate frame. It is computationally convenient, therefore, to generate the refractivity gradient in spherical coordinates $(r,\theta,\alpha)$, which can be converted into local curvilinear coordinates $(u,v,w)$ using the following transformation.

$$[\nabla n]_{rm} = \frac{\partial n}{\partial r}u + \frac{1}{r\sin\alpha}\frac{\partial n}{\partial\theta}v + \frac{1}{r}\frac{\partial n}{\partial\alpha}w \qquad (2\text{-}7)$$

A further rotational transformation is then applied to the local curvilinear coordinate frame to give the gradient in a fixed cartesian frame $(x,y,z$ in Fig. 2-1) suitable for numerically solving equations 2-5 and 2-6.
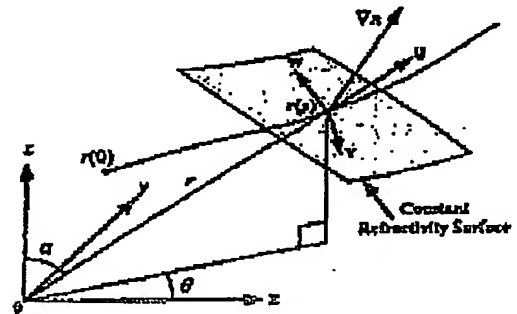


Fig. 2-1  Refractivity Geometry

The tropospheric delay can be computed as:

$$d_{trop} = \int_a^b n(s)\,ds + \int_b^c ds - \int_b^c ds \qquad (2\text{-}8)$$

where   a, b and c are as shown in Fig. 2-2. Point b corresponds to the point at which ray curvature and refractivity is negligible, in this work assumed to be above an altitude of 70km.
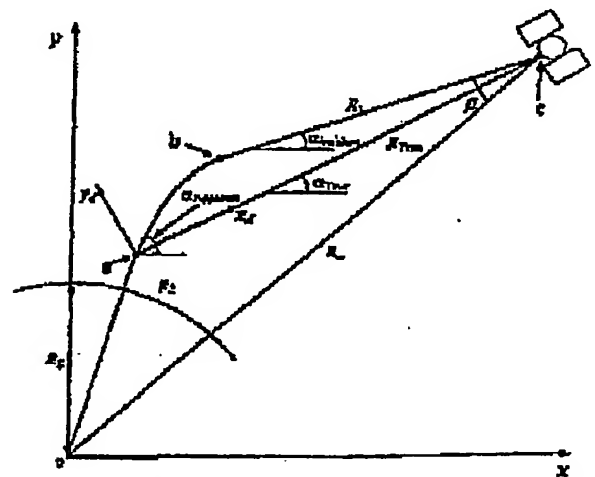


Fig. 2-2  Ray Path Geometry

## 2.2 Example Propagation Paths

An example propagation path for a satellite at an elevation of $5°$ is shown in Fig. 2-3. The co-ordinates used are $x_d$ and $y_d$ as shown in Fig. 2-2. It is noted that

6

majority of the curvature of the ray-path occurs 100-km from the user. It is the rotation of the refractivity gradient vector field, caused by earth curvature, which is the dominant cause of ray curvature; rather than the rate of change of refractivity scalar field. The apparent elevation angle, the propagation path angle at the user location, is approximately $5.19°$ for a true elevation angle from satellite to user of $5°$.

It is shown, in Fig. 2-3, that an extreme ionosphere (TEC =100) does not result in a significant change in ray angle on entry into the troposphere therefore, the assumption of the addition of troposphere to ionospheric delays is valid as the coupling effect is minimal.
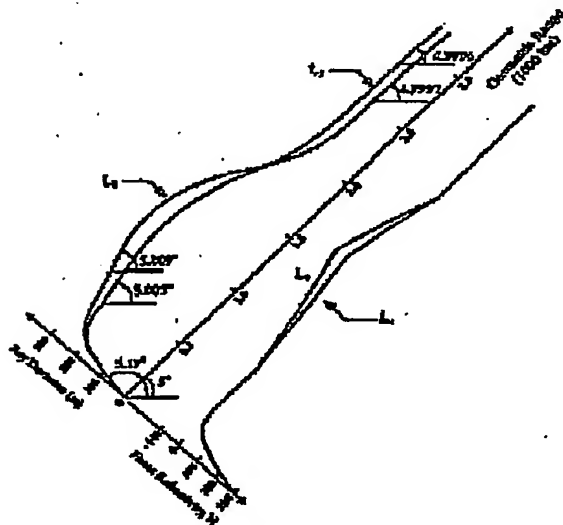


Fig. 2-3 Example Ray Deviation at $5°$.

Example delays and additional path length due to ray curvature are given in Fig. 2-4. The increase in path length due to curvature is approximately 19cm for a satellite at $5°$ elevation.
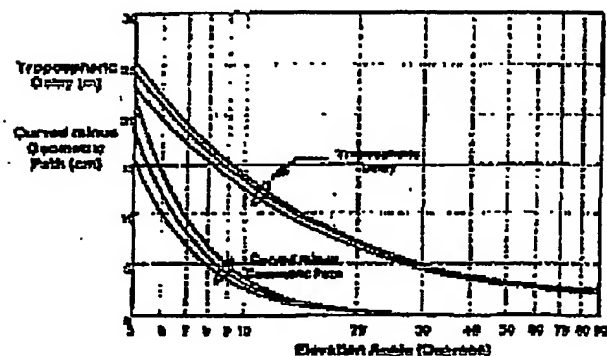


Fig. 2-4 Example Delay and Excess Curved Path

## 2.3. Equivalent Angle Approximation

The method of determining the tropospheric delay, by numerically solving a system of ordinary differential equations, is computationally expensive. A faster method is to integrate the refractive index along a straight geometric path; however this integration will result in an overestimation of tropospheric delay; in reality the ray bends so as to minimise the propagation time (Fermat's principle).

There exists an equivalent elevation angle, lying between the true (geometric) and apparent elevation angle, that results in the straight path integral being equal to the integral along the actual curved path from satellite to user. The elevation correction to be added to the true elevation to obtain the equivalent angle, varies with user altitude, but is largely unchanged with atmosphere (Fig. 2-5). The standard deviation between the equivalent straight line integral and the ray-traced tropospheric delays for elevations between 3 and 10 was found to be approximately 0.04%.
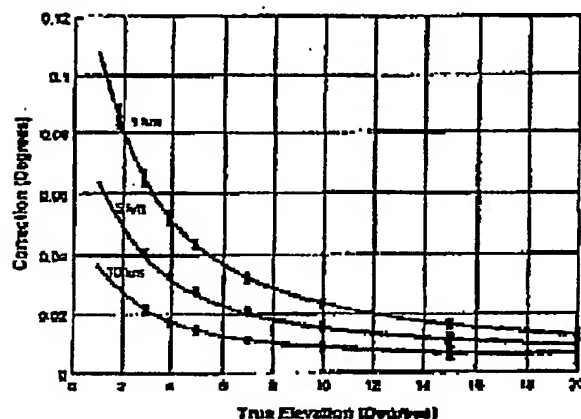


Fig. 2-5 Correction to True Elevation Angle.

## 3. NUMERICAL WEATHER FIELD PROCESSING

### 3.1 Introduction

Numerical Weather Prediction models forecast the evolution of atmospheric physical processes by applying governing equations, including the conservation of mass, momentum and energy. Three-dimensional fields of continuous variables including humidity, pressure, temperature and velocity are numerically processed and meteorological features, including weather fronts, are secondary derived properties. A variety of measurements can be input into the numerical model including surface, radiosonde and satellite observations. The water cycle is modelled including the effects of

...ain moisture, sea surface temperature, cloud ...ation and precipitation.

There are a variety of co-ordinate systems in use for numerical weather prediction; they can be either based upon a grid of fixed points or spectral coefficients. Physical height is rarely used as the vertical co-ordinate in NWP: pressure, sigma-pressure and hybrid co-ordinates are more convenient. Sigma-pressure vertical co-ordinates define a level to be a surface of constant pressure divided by surface pressure and thus have a terrain following property. Hybrid co-ordinates are terrain following at low levels, but tend continuously to pressure surfaces at upper levels.

Numerical models can be global or of limited area. Limited area high-resolution models are often termed mesoscale models as they reflect mesoscale meteorological features: weather patterns of less than 100km in size.

### 3.2 Mesoscale Resolution Model

The mesoscale data used in this study was obtained from the British Atmospheric Data Centre with permission from the United Kingdom Meteorological Office, UKMO. The UKMO mesoscale Unified Model uses a hybrid vertical co-ordinate system with a spatial resolution of 12×12 km. The model covers the area shown in Fig. 4-2. Specific humidity is modelled at 35 hybrid levels; temperature is modelled at 38. To ray-trace through the numerical weather field the hybrid levels are converted into physical height by assuming hydrostatic equilibrium. The impact of deviations from hydrostatic equilibrium caused by mountainous terrain on lunar laser range measurements has been estimated to be less than 1cm for elevation angles as low as 20° [8], the impact due to convective storms is not known. In assuming hydrostatic equilibrium, local values for gravity are used to reflect gravitational variation with latitude and altitude.

Once the NWP fields are fixed in 3-D space, the data can be re-sampled, using a combination of linear and log-linear interpolation, at any physical height. The atmosphere was extrapolated from the top of the NWP field (approximately 35km) to an altitude of 70km assuming a log-linear relationship between refractivity and altitude. The atmosphere can then be represented as a refractivity field, from which the refractivity gradient is numerically computed.

### 3.3 Atmospheric Refractivity

The atmospheric refractivity can be derived from atmospheric pressure, water vapour partial pressure and temperature fields. Atmospheric refractivity can be divided into dry (hydrostatic) and wet components. A simple two-term expression, given in [2], has a refractivity accuracy of 0.5%:

$$N = N_{dry} + N_{wet} = \frac{77.6}{T}\left(P + 4810\frac{e}{T}\right). \qquad (3\text{-}1)$$

$$N = 10^{6}(n-1) \qquad (3\text{-}2)$$

where:

$N$ is the refractivity.
$P$ is atmospheric pressure (millibar)
$E$ is the water vapour pressure (millibar)
$T$ is temperature (Kelvin)

A review of more sophisticated three-term expressions including gas compressibility effects, possessing greater accuracy, is given in [5].

### 3.4 Future Numerical Weather Prediction

The rapid improvement in computational power and advances in numerical techniques has seen the ECMWF model's horizontal spatial resolution reduce from 200km to 26km in the period 1979-2001. This process is expected to continue and it is predicted that by 2015 limited-area model resolution could be 1km and the global model less than 10km [11].

## 4. MESOSCALE METEOROLOGICAL FEATURES

### 4.1 Relevant Meteorological Features

Meteorological features that possess a large spatial and/or temporal variation in tropospheric delay will impact the accuracy of NWP-derived tropospheric corrections and the bandwidth required for dissemination. The temporal and spatial variation in hydrostatic refractivity is generally small, whereas meteorological features associated with rapid changes in atmospheric moisture significantly impact the accuracy/bandwidth relationship.

The spatial and temporal scales of certain weather systems are described in Fig. 4-1 (from [1]). Meteorological features smaller than the resolution of the numerical prediction model will not be accurately reflected in the NWP-derived tropospheric correction. The 12×12 km resolution fields are able to reflect characteristics of weather fronts, however smaller features such as local storms and tornadoes would not be well represented spatially or temporally. The extent of the weather features in altitude is critical in assessing their relevance to tropospheric delay anomalies.
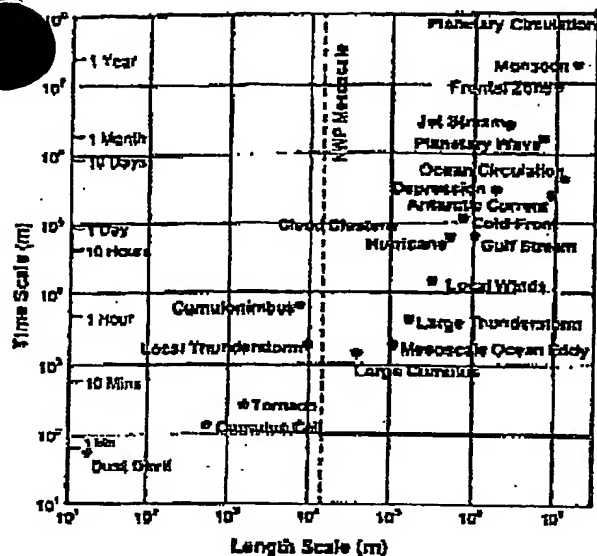
Fig. 4-1  Spatial Scale and Life Span of
Meteorological Systems [1]



Fig. 4-2  Synoptic Chart Weather Front Feature

## 4.2  Weather Fronts

A weather front marks the interface between air masses
defined as a large body of air whose physical properties
are largely uniform horizontally for hundreds of
kilometres. The front can mark the occurrence of abrupt
changes in atmospheric moisture, temperature and
therefore refractivity.  Fronts can be divided into three
classifications: warm, cold and occluded.

Each frontal zone is unique however they do posses
some general characteristics. Frontal zones tend to have
a width of a few 10kms.  A warm front represents the
leading edge of an advancing warm air mass, and
generally has a gentle slope (inclination), typically 0.5 -
1°.  Cold fronts, the leading edges of advancing cooler
air masses, are typically inclined at 2°.  Another
characteristic of the front is its relative speed, cold fronts
move much faster than warm fronts, up to 50km/hr
compared to 10km/hr respectively.  Hence, when a cold
front catches up with a warm front it undercuts the
warmer less dense air and the resultant, more complex,
feature is termed an occluded front.  Occluded fonts
contain characteristics that belong to both cold and warm
fronts.

The most rapid change in tropospheric delay is likely to
occur when satellite elevation and front inclination are
equal. Generally, in the UK, frontal systems move at 30
to 50 kilometres per hour and can result in zenith delay
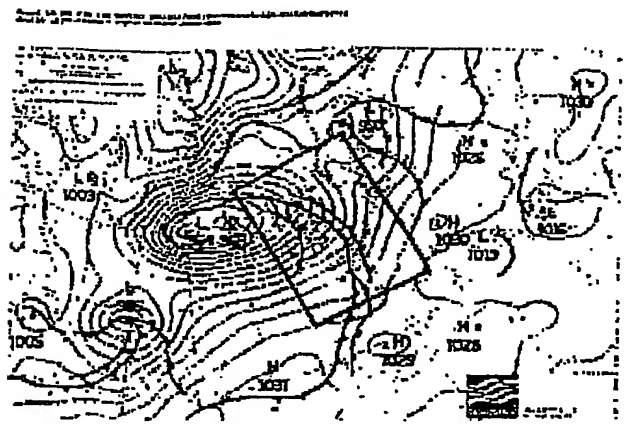variations of 3cm/hour [12].



Fig. 4-3  Meteosat Image 19/01/2002

An example of a weather frontal system is shown in the
synoptic chart in fig. 4-2 (obtained from the
Wetterzentrale website).  The system, within the
highlighted Unified Model coverage area, includes
occluded, cold, warm and elevated cold fronts.  The
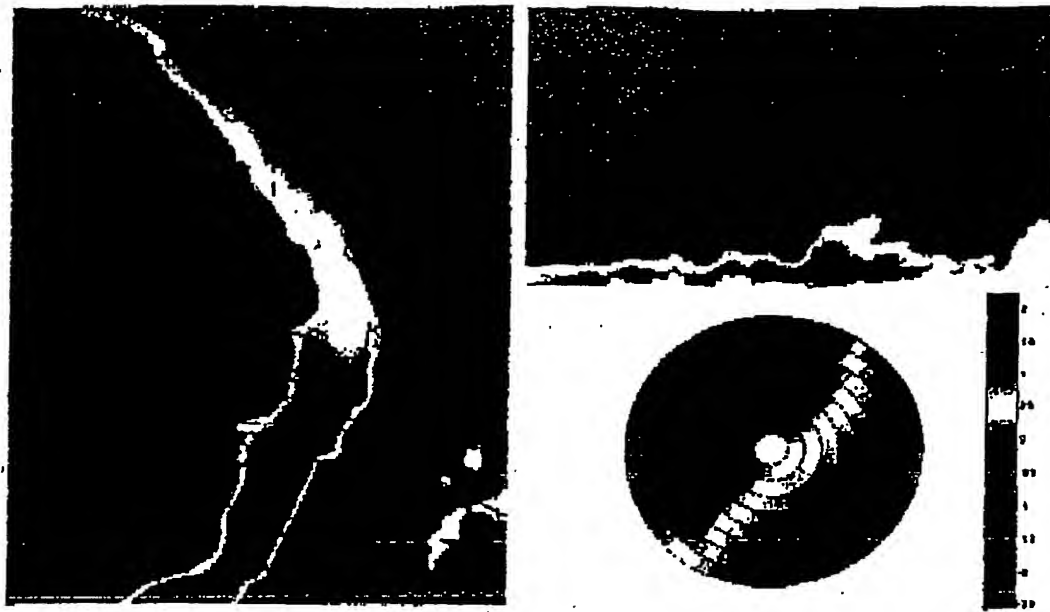frontal system is associated with abrupt changes in

9

Fig. 5-1  Azimuthal Asymmetry Feared Event

atmospheric moisture content, which can be seen as an abrupt change in cloud coverage, Fig. 4-3, a Meteosat image obtained from Dundee University; and specific humidity, Fig. 5-1, a NWP mesoscale image.

## 5.  AZIMUTHAL ASYMMETRY

The accuracy of the widespread assumption that the atmosphere is symmetric in azimuth can be tested by examining the variation in tropospheric delay for a given elevation angle.  A data set, comprising UKMO mesoscale NWP fields in two-hourly intervals for the 1[x] and 15th of each month over a period of one year, was used to generate azimuthal asymmetry amplitude statistics.  Four user locations were used near the mesoscale region centre: each location was tested in increments of 10 degrees of azimuth at an altitude of 500m above mean-sea-level.  Fig. 5-2 shows the percentage variation in tropospheric delay from the mean delay for elevation angles of 2, 5, 10 and 20°.  The standard deviation of azimuthal asymmetry expressed as a percentage for each elevation is 0.21, 0.12, 0.07 and 0.03% respectively.  The amount of azimuthal asymmetry is small in relation to the current accuracy of the NWP-derived tropospheric corrections: a standard deviation of 0.4%. For users requiring the highest degree of accuracy, azimuthal asymmetry information would be of value, however for most users, the cost of disseminating azimuthal asymmetry information outweighs the small gain in accuracy. As the accuracy of NWP-derived corrections improves, mainly due to

improved model resolution, azimuthal asymmetry is likely to become a more significant limiting factor.
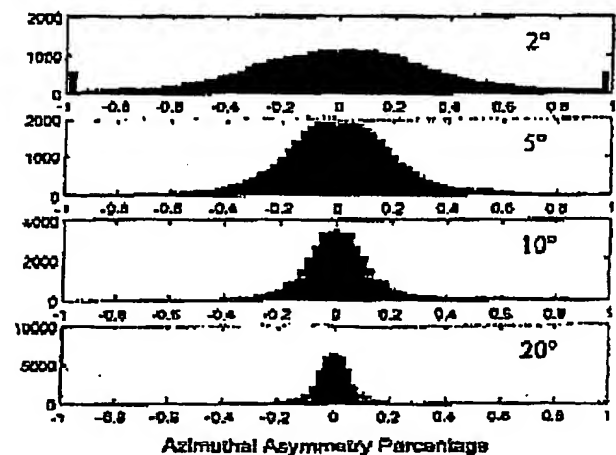


Fig. 5-2  Azimuthal Asymmetry Histogram

The distribution of the measure of asymmetry has long tails.  Extreme levels of asymmetry occur when a weather front is overhead.  Fig. 5-1 consists of a specific humidity horizontal slice at an altitude of 2km, a specific humidity vertical slice and polar plot indicating the percentage of azimuthal asymmetry.  The polar plot displays the percentage change in delay from the mean delay for that elevation. The concentric rings are for

10

...ion angles of 1, 2, 3, 4, 5, 7, 10 and 15°. The on of asymmetry caused by simple weather fronts oc accurately modelled as a sinusoid. Sinusoid parameters could than used by users requiring the highest accuracy of tropospheric corrections, as suggest in [7].

## 6. ELEVATION MAPPING

In modelling tropospheric delay it is convenient to relate the tropospheric delay at a given elevation angle to the zenith delay ($d_{Trop}^z$) by means of a mapping function (m(el)).

$$d_{Trop} = d_{Trop}^z m(el) \qquad (6\text{-}1)$$

The hydrostatic zenith delay can be accurately modelled given a surface pressure measurement [6], however the wet zenith delay can not be accurately determined from surface humidity measurements, as they are not representative of the above atmosphere. The expression for the tropospheric delay at a given elevation angle can be defined as:

$$d_{Trop} = d_{hyd}^z m_{hyd}(el) + d_{wet}^z m_{wet}(el) \qquad (6\text{-}2)$$

It is noted that care must taken when applying the simplification of the superposition of hydrostatic and wet atmospheric delays: the propagation path is dependent upon both hydrostatic and wet components.

The variation of tropospheric delay with elevation angle (Fig. 2-4) can be efficiently modelled by a continued fraction expansion. Niell hydrostatic and wet mapping functions [10] possess a high degree of accuracy without the need for prior meteorological information. Niell mapping functions use a continued fraction function based on three parameters a, b and c, which are a function of time of year, latitude and altitude. Niell mapping functions are likely to result in significant additional errors compared to the accuracy of NWP-derived zenith corrections. A more accurate direct mapping function can be used based upon NWP ray-traced results [4].

For the reasons of dissemination efficiency, it was decided to use a three-term continued fraction approximation to the total (wet and dry) mapping function determined from ray tracing NWP fields (equation 6-3). Parameters $a_0$, $b_0$ and $c_0$ amount to an a priori Niell mapping function for the total (hydrostatic and wet) tropospheric delay, and are a function of time of year, latitude and altitude. The parameters $\Delta a$, $\Delta b$, and $\Delta c$ are a correction term to be broadcast. The correction parameters are determined from a fitting process such that the sum of the squares of the residuals between equation (6-3) and the ray-traced (truth) is minimised.

Such an approximation was found to be in agreement with the ray-traced results (typically <<0.1% residual error).

$$m(\varepsilon, a, b, c) = \cfrac{1 + \cfrac{a_0 + \Delta a}{1 + \cfrac{b_0 + \Delta b}{1 + c_0 + \Delta c}}}{\sin(\varepsilon) + \cfrac{a_0 + \Delta a}{\sin(\varepsilon) + \cfrac{b_0 + \Delta b}{\sin(\varepsilon) + c_0 + \Delta c}}} \qquad (6\text{-}3)$$

## 7. SPATIAL AND TEMPORAL VARIABILITY

The rate of information required to accurately disseminate tropospheric correction information, on a regional basis, is dependent upon the spatial and temporal variation of tropospheric delays.

### 7.1 Temporal Resolution

The impact of temporal resolution on the accuracy of NWP-derived tropospheric corrections can be analysed by comparing the change in zenith delay at time $t_0$ and $t_0 + \Delta t$. Using the data set as used for the azimuthal asymmetry analysis, the changes in zenith delay were computed for $\Delta t$ values of 1, 2, 4 and 8 hours for all points in the NWP coverage area. The standard deviation of temporal variation, expressed as a percentage for each $\Delta t$ value, is 0.475, 0.594, 0.798 and 1.068% respectively. The corresponding histograms are given in Fig. 7-1.
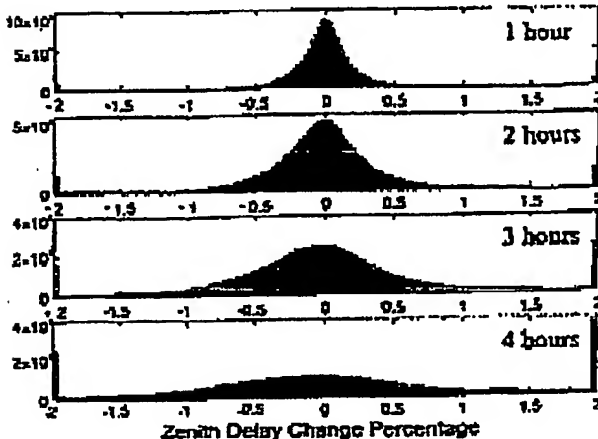


Fig. 7-1 Temporal Resolution Histogram

The impact of temporal resolution is significant in relation to the current accuracy of the NWP-derived tropospheric corrections: a standard deviation of 0.4%.

11

Fig. 7-2 Front Progression

A significant error additional error is therefore produced if temporal resolution exceeds 1 hour.

The distribution of the temporal variation has long tails. Fig. 7-2 displays the percentage change in zenith delay, for Δt values of 1, 2, and 4 hours, as a weather front traverses the UK. The weather front has resulted in a maximum rate of change of zenith delay of 4cm/hour (1.6%) measured between $t_0$ and $t_0 + 1$ hour.

## 7.2 Spatial Resolution

The impact of spatial resolution on the accuracy of NWP-derived tropospheric corrections can be analysed by comparing the change in zenith delay for locations separated by fixed distances. Using the data set as used for the azimuthal asymmetry analysis, the changes in zenith delay were computed for spatial separations of 1, 2, 4 and 8 mesoscale grid points in North and East directions (equivalent to 12, 24, 48 and 96km separations). The standard deviations of spatial variation, expressed as a percentage for each spatial separation value, are 0.138, 0.213, 0.352 and 0.576% respectively. The corresponding histograms are given in Fig. 7-2. Spatial resolutions, larger than the resolution of the mesoscale model, 12 km, are therefore found to result in significant addition tropospheric errors. The spatial variation in tropospheric zenith delay has a close relationship to temporal variation. As a weather front passes over, for example at 40 km/hour in the east direction, the difference in zenith delay observed at $t_0$ and $t_0+1$ hour is similar to that observed between two points separated by 40 km in the east/west direction.
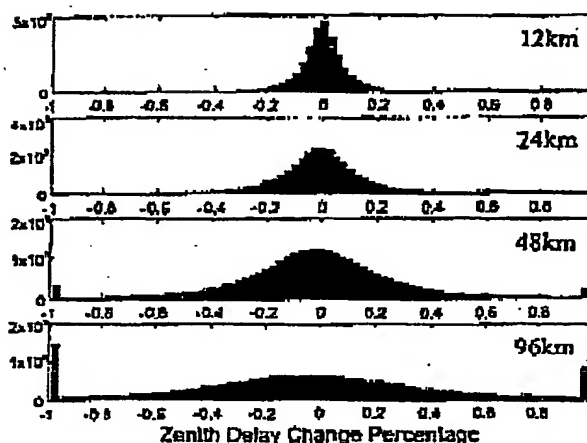


Fig. 7-3 Spatial Resolution Histogram

## 8. BANDWIDTH REQUIREMENTS

### 8.1 Quantisation

To achieve efficient tropospheric correction dissemination, it was decided not to model the atmosphere, for example with pressure, humidity and lapse rate information, but to supply the minimum information needed for accurate delay determination. Similarly, for reasons of bandwidth efficiency, zenith delay and mapping function parameters can be expressed as corrections to a priori models. The zenith delay, disseminated as a percentage correction to the RTCA model [9], can be coded using 8 bits spanning the range -10% to +10% (consistent with [13]) with a resolution of 0.0781% and therefore minimal quantistion noise. Similarly, mapping function continued fraction information can be disseminated as a correction to a Niell-like total delay mapping function. It is proposed
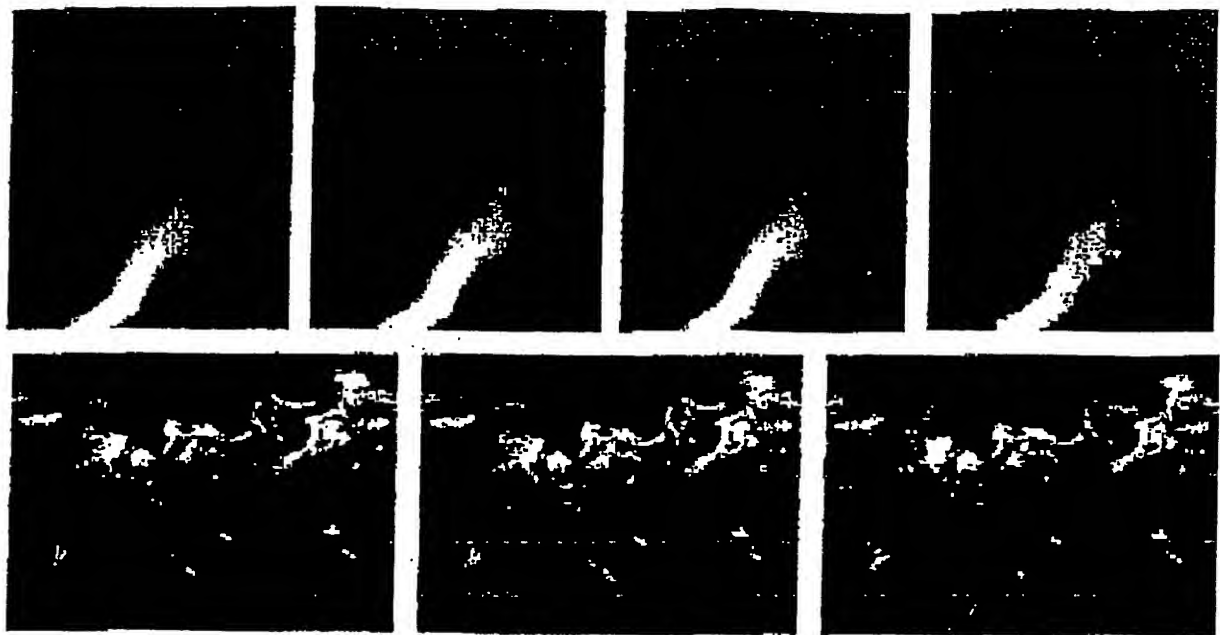
Fig. 8-1 Zenith Delay Image Compression

that mapping function correction parameters can be adequately described by 16 Bits (7, 5 and 4 for parameters $\Delta u$, $\Delta b$ and $\Delta c$, Equation 6-3).

## 8.2 Image Compression

To investigate the impact of quantisation and compression on the accuracy of disseminated tropospheric delay corrections, an example zenith delay map derived from UKMO mesoscale NWP fields, with an active front, was quantised and compressed. The accuracy of the recovered (disseminated) correction was then compared to the original values: derived from ray-traced numerical weather prediction fields. The resultant greyscale bitmap image, 146×182×8 Bits, and three JPEG images, with successively increasing compression ratios, are shown in the first four images of Fig. 8-1. The size of the 8-bit bitmap image, a zipped (loss-less compression) bitmap, and three JPEG images are shown in Table 8-1.

| Type | Size Bytes | Comp. Ratio | Noise (std) | Worst Value |
|---|---|---|---|---|
| BMP | 28014 | 1 | 0.023% | 0.05% |
| Zipped BMP | 11212 | 2.5 | 0.023% | 0.05% |
| JPEG90 | 2318 | 12.1 | 0.042% | 0.3% |
| JPEG50 | 1139 | 24.6 | 0.093% | 0.5% |
| JPEG10 | 734 | 38.2 | 0.28% | 2.5% |
| Sub-sampling | | 4 | 0.035% | 0.35% |
| Sub-sampling | | 16 | 0.063% | 0.5% |

| | | 25 | 0.081% | 0.5% |
|---|---|---|---|---|
| Sub-sampling | | | | |

Table 8-1 Compression Properties Mesoscale

The bitmap (BMP) and zipped bitmap results in a quantisation noise of 0.23%. The JPEG50 image has compressed the bitmap image by a factor of 24.6, but the additional quantisation and compression noise is small, less than 0.1%, compared to the current accuracy of NWP-derived correction (0.4%). It is noted however that simple under-sampling every fifth pixel, then using bilinear interpolation between missing pixels, results in a compression factor of 25 and less noise than JPEG50: for this image JPEG image compression offers no advantage over a reduced sampling rate. Further compression resulted in substantial reduction in performance as can been seen in Fig. 8-1.

| Type | Size Bytes | Comp. Ratio | Noise (std)* | Worst Value |
|---|---|---|---|---|
| BMP | 141478 | 1 | 0.025% | 0.07% |
| Zipped BMP | 80404 | 1.8 | 0.025% | 0.07% |
| JPEG90 | 20195 | 7 | 0.089% | 1.2% |
| JPEG50 | 8457 | 16.7 | 0.17% | 1.8% |
| Sub-sampling | | 4 | 0.17% | 3.3% |

*Note: noise standard deviation is area weighted

Table 8-2 Compression Properties Global

13

Fig. 8-2   Example Zenith Delay Relative to RTCA Model (%) using UKMO Global Model

An example UKMO global NWP greyscale bitmap image and two JPEG images, with successively increasing compression ratios, are shown in the last three images of Fig. 8-1. The original zenith delay, expressed as a percentage change from the RTCA model, is shown in Fig. 8-2. The global model has a resolution of 5/6 and 5/9 degrees in longitude and latitude respectively: producing a global image of 432×325×8 Bits. The JPEG90 image compresses the bitmap image by a factor of 7 (Table 8-2) with compression noise of less than 0.1%; the JPEG50 image results in significant additional zenith delay errors as can be seen in Fig. 8-1. For the global image the sub-samping technique, with a compression factor of 4, results in substantial additional compression errors.

Assuming that mapping function parameter corrections can be similarly compress .......
*** Bandwidth e.g. 200 Bit/s global data disseminated in 10 minutes ***

## 9. SUMMARY CONCLUSIONS

An accurate atmospheric refractivity profile, and therefore tropospheric delay, is simply a by-product of the numerical weather prediction process. A vector calculus based approach reduces the problem of propagation path determination, through the numerical weather prediction derived refractivity field, to the solution of a system of ordinary differential equations suitable for solving by numerical methods.

The accuracy of tropospheric corrections used by a satellite navigation user is dependent upon the accuracy of the numerical weather prediction (currently 0.4% standard deviation for the UKMO mesoscale model) and

on the error introduced due to process of correction dissemination.

For the data set used in this study, errors due to the omission of azimuthal asymmetry effects were found to be small in comparison with numerical weather prediction errors. Only for users requiring the highest degree of accuracy would azimuthal asymmetry information be of value. The impact of temporal resolution is significant in relation to the current accuracy of the NWP-derived tropospheric corrections. A significant additional error is therefore produced if temporal resolution exceeds 1 hour. Spatial resolutions, larger than the resolution of the mesoscale model, 12 km, are therefore found to result in significant additional tropospheric errors.

For reasons of bandwidth efficiency, zenith delay and mapping function parameters can be expressed as corrections to a priori models. 8 Bits can used to describe tropospheric zenith delay with minimal quantisation noise; a further 16 Bits may be required to disseminate the elevation mapping function expressed as continued fraction correction parameters.

The tropospheric correction maps can be compressed with minimal reduction in image performance, but a substantial decrease in data size. A combination of efficient quantisation and compression techniques results in the data-rate for tropospheric correction dissemination being suitable for transmission via Global Naviagtion Satellite Systems.

The zenith delay and mapping function parameters can be used in assisting the process satellite orbit determination.

14

## 10. REFERENCES

1. Barry, R. G., Chorley R. J., "Atmosphere Weather and Climate", Seventh Edition 1998, ISBN 0-415-16020-0

2. ITU-R P.453-6 "The Radio Refractive Index: Its Formula and Refractivity Data".

3. Born, M., Wolf, E., "Principles of Optics", Sixth Edition 1980, ISBN 0-08-026482-4.

4. Rocken, C., Sokolovskyiy, S., Johnson, J. M. & Hunt, D., "Improved Mapping of Tropospheric Delays", Journal of Atmospheric and Oceanic Technology, Volume 18, 2001.

5. Davis, J. L., Herring T. A., Shapiro, I. I., Rogers, A. E. E. and Elgered G., "Geodesy by radio interferometry: Effects of atmospheric modelling errors on estimates of baseline length", Radio Science, Volume 20, Number 6, Pages 1593-1607, Nov-Dec 1985.

6. Saastamoinen, J., "Atmospheric correction for the troposphere and stratosphere in radio ranging of satellites. The Use of Artificial Satellites for Geodesy, Geophys. Monogr. Ser., pp 247-251, 1972.

7. Chen, G., Herring, T. A., "Effects of atmospheric azimuthal asymmetry on the analysis of space geodetic data", Journal of Geophysical Research, Vol. 102, No. B9, Pages 20,489-20,502, September 1997.

8. Hauser, J. P., "Effects of Deviations from Hydrostatic Equilibrium on Atmospheric Corrections to Satellite and Lunar Laser Range Measurements", Journal of Geophysical Research, Vol. 94, No. B8, Pages 10,182-10,186, August 1989.

9. RTCA DO229C, "Minimum Operational Performance Standards for Global Positioning System / Wide Area Augmentation System Airborne Equipment", November 2001.

10. Niell A. E., "Global mapping functions for the atmosphere delay at radio wavelengths", Journal of Geophysical Research, Vol. 101 No. B2, Pages 3227-3246, February 1996.

11. Schär, C., "Alpine Numerical Weather Prediction 2000-2020: A look Back to the Future", Map Newsletter, No. 14, March 2001.

12. Gregorius, T., Blewitt, G., "The Effect of Weather Fronts on GPS Measurements", GPS World, Innovation, May 1998.

13. Collins, J. P. and Langley, R. B., "The residual tropospheric propagation delay: How bad can it get?", Proceeding of ION GPS1998.

TOTAL P.12

## CLAIMS

1.    A method of obtaining data for use in a satellite positioning system or GNSS comprising the steps of generating a first set of less accurate tropospheric delay values from a first model which is known per se, the first model being based on a first set of parameters, generating a second set of more accurate tropospheric delay values from a second model based on meteorological information, and developing a modified said set of parameters for use with said first model so that it then provides a set of delay values substantially approximating the second set, and expressing at least one of said modified set of parameters as a correction parameter for communication to a user.

2.    A method according to claim 1 wherein said first set comprises tropospheric zenith delays.

3.    A method according to claim 2 wherein the first model contains a mapping function relating tropospheric delay at a given elevation angle to the zenith based on methodology used by Neil to derive a parametric model of the tropospheric delay to satellites observed by the user.

4.    A method according to any preceding claim wherein the first model is based on non-meteorological parameters.

5.    A method according to claim 4 wherein said non-meteorological parameters comprise one, or any two, or all three of time of year, latitude and altitude.

6.    A method according to any preceding claim wherein said second model is based on NWP data.

7.    A method according to any preceding claim wherein said second set is derived by a ray tracing technique.

8.    A method according to claim 7 wherein parameters generated in the first model are generated in the second model from the ray tracing data and the differences are determined for a geographical region.

16

9. A method according to claim 7 or claim 8 wherein a distribution of said correction parameters over at least part or all of the earth's surface is derived for communication to at least one geostationary or non-geostationary satellite.

10. A method according to claim 9 wherein said distribution is subject to data reduction to enable a low capacity communications channel or data link to be used.

11. A method according to claim 10 where said data reduction is performed using lossy image compression or sub-sampling techniques.

12. A method according to claim 10 or claim 11 and including the step of transmitting the reduced data over a communications channel or data link.

13. A method according to claim 12 wherein the amount of data reduction is sufficient to permit said transmission within a time substantially lower than the validity time of the said meteorological information.

14. A method according to claim 12 wherein the NWP data defines a cell size, and if the standard deviation for the change in zenith delay for a cell over a period t equals the inaccuracy in the said second set, then the data reduction is effective to reduce the data to an amount which can be transmitted over a bandwidth of 200 bit per second in a time $t'$ substantially less than $t$.

15. A method according to claim 12 wherein $t'$ is no more than $t/4$.

16. A method of any one of claims 12 to 15 wherein said communications channel or data link is to a geostationary or non-geostationary satellite.

17. A method according to claim 16 wherein said geostationary or non-geostationary satellite re-transmits at least part of said distribution to a user.

18. A method according to any preceding claim wherein the or each said correction parameter is expressed as the difference between the parameter of said first set and the parameter of said modified set.

17

19.     Apparatus of obtaining data for use in a satellite positioning system or GNSS comprising first generating means for generating a first set of less accurate tropospheric delay values from a first model which is known per se and which is based on non-meteorological parameters, second generating means for generating a

5     second set of more accurate tropospheric delay values from a second model based on meteorological information, and developing means for developing a set of modified said parameters for use with said first model so that it then provides a set of delay values substantially approximating the second set, and said developing means being arranged to express the modification to said first parameters as a set of correction

10    parameters.

20.     Apparatus according to claim 19 and including means for compressing said set of correction factors.

21.     Apparatus according to claim 19 or claim 20 and comprising transmission means for transmitting said set or said compressed set of correction factors to a user

15    via a geostationary or non-geostationary satellite.

18